

Frequency Comparison of Two $^{40}\text{Ca}^+$ Optical Clocks with an Uncertainty at the 10^{-17} Level

Y. Huang,^{1,2} H. Guan,^{1,2,*} P. Liu,^{1,2} W. Bian,^{1,2} L. Ma,³ K. Liang,⁴ T. Li,⁴ and K. Gao^{1,2,5,†}

¹State Key Laboratory of Magnetic Resonance and Atomic and Molecular Physics, Wuhan Institute of Physics and Mathematics, Chinese Academy of Sciences, Wuhan 430071, China

²Key Laboratory of Atomic Frequency Standards, Wuhan Institute of Physics and Mathematics, Chinese Academy of Sciences, Wuhan 430071, China

³East China Normal University, Shanghai 200062, China

⁴National Institute of Metrology, Beijing 100013, China

⁵Center for Cold Atom Physics, Chinese Academy of Sciences, Wuhan 430071, China

(Received 13 June 2015; published 6 January 2016)

Based upon an over-one-month frequency comparison of two $^{40}\text{Ca}^+$ optical clocks, the frequency difference between the two clocks is measured to be 3.2×10^{-17} with a measurement uncertainty of 5.5×10^{-17} , considering both the statistic (1.9×10^{-17}) and the systematic (5.1×10^{-17}) uncertainties. This is the first performance of a $^{40}\text{Ca}^+$ clock better than that of Cs fountains. A fractional stability of 7×10^{-17} in 20 000 s of averaging time is achieved. The evaluation of the two clocks shows that the shift caused by the micromotion in one of the two clocks limits the uncertainty of the comparison. By carefully compensating the micromotion, the absolute frequency of the clock transition is measured to be 411 042 129 776 401.7(1.1) Hz.

DOI: 10.1103/PhysRevLett.116.013001

Great improvements have been made with optical clocks in recent years, with both single trapped ions [1–5] and neutral atoms [6–13]. For most of the above-mentioned optical clocks, the uncertainties are found to be better than that of the state-of-art Cs primary standard [14,15] by which the accuracy of SI second is currently realized. Scientists are expecting to make a new definition of SI time unit using high-accuracy optical clocks [16,17]. During the development of an optical clock, it is convenient to set up two clocks, and their comparison can be used for testing both the stability and the reproducibility. Furthermore, we can check the systematic evaluation from the comparison of two clocks. The comparison of optical clocks has been performed with the same kind of atoms or ions [3,6–8,12,18] and different kinds [19–21]. Recently, the constraints on a possible temporal variation of fundamental constants were improved by the comparison between two different transition frequencies using the same single Yb ion, together with Cs fountains [22,23]. The clocks with the best stability today are based on neutral atoms in optical lattices. The Sr clock developed in JILA and the Yb clock developed in NIST achieved stability at a few parts in the 10^{-18} level at $\sim 10\,000$ s [6,7,12]; for the Sr clock in the University of Tokyo, similar performances have been achieved by comparing two cryogenic clocks synchronously [8]. For the ion-based optical clocks, the best stability achieved is $2.0 \times 10^{-15}/\sqrt{\tau}$, with the comparison of two Al^+ quantum logic clocks [1].

Optical clocks based on $^{40}\text{Ca}^+$ ions have been studied recently by the University of Innsbruck [24], National

Institute of Information and Communications in Japan (NICT) [21], and Wuhan Institute of Physics and Mathematics in China (WIPM) [25,26]. The $^{40}\text{Ca}^+$ optical clock has its own advantages. Its simplicity on the laser system allows the possibility of making a low-cost, compact, and robust optical clock. However, there is no experimental comparison between $^{40}\text{Ca}^+$ optical clocks with agreement below 1 part in 10^{16} to date, which could prove that the $^{40}\text{Ca}^+$ optical clocks also have better stability and uncertainty than that of Cs fountains. In this Letter, we report the comparison between two $^{40}\text{Ca}^+$ optical clocks with a total fractional uncertainty of 5.5×10^{-17} , including both the statistic and systematic uncertainties. The frequency difference between two clocks is within the uncertainty. Besides, the systematic uncertainties for both clocks are evaluated to be better than 6×10^{-17} , which is one order of magnitude smaller than the previous evaluation for our first clock [26]. A fractional stability of 7×10^{-17} in 20 000 s of averaging time is achieved for both clocks. Furthermore, after carefully evaluating all the possible systematic shifts, the absolute frequency of the clock transition is measured to be 411 042 129 776 401.7 (1.1) Hz, with measurements relative to a maser referenced to the SI second via UTC(NIM) through GPS.

Our two $^{40}\text{Ca}^+$ optical clocks are based on the $4s_{1/2} \rightarrow 3d_{5/2}$ electric quadrupole transition at 729 nm. The two ions are both trapped with miniature Paul traps [25]—one of the traps is driven at $\sim 2\pi \times 9.6$ MHz; the other is driven at $\sim 2\pi \times 24.7$ MHz at which the rf-induced Stark shifts and 2nd-order Doppler shifts cancel each other [2,27]. The

ambient magnetic field is reduced by two layers of magnetic shielding and then minimized with three pairs of compensating coils. A background magnetic field of $\sim 0.5 \mu\text{T}$ is applied to split the Zeeman components. Each clock laser beam passes through an acousto-optic modulator (AOM) to match the clock transition. When locked to the ion, the AOM driving frequencies for both clocks are recorded, from which we can calculate the clock frequency difference. For cancellation of the linear Zeeman shift, the quadrupole shift, and the tensor part of the Stark shifts [28], the locking scheme is similar to the previous work [25], except a much longer probe pulse is chosen to improve the stability. The clock laser synchronously probes two ions in the two traps with a probe pulse time of 40–80 ms, which leads to an observed 10–20 Hz Fourier-transform-limited linewidth.

Comparing to our previous work, the photon-ionization technique is used instead of electron bombardment, which greatly reduces the contamination of the trap caused by the large atom and electron flux. The micromotion drift is greatly reduced by this technique. Normally, one or two days after the loading, the micromotion becomes stable and the ion can be trapped for tens of days continuously. The stability of the clock laser is also greatly improved comparing to the previous result [29]. After introducing the power stabilization, the fiber noise cancellation, the passive control of the residual amplitude modulation, and the optimization of the servo circuits, the noises caused by the above sources are all below the thermal noise, which is the fundamental limit for the frequency stability achieved with a rigid frequency reference cavity due to the Brownian motion of the cavity material at room temperature [30]. Comparing with another 729 nm laser of similar performance, the stability is measured to be $< 2 \times 10^{-15}$ at 1–30 s; and the linewidth is measured to be < 1 Hz at ~ 3 s. The long-term isothermal drift is measured to be ~ 60 mHz/s, which is compensated using an AOM. Two 10-m-long fibers used for probing both traps are also phase-noise canceled. By increasing the probe time to 200 ms, a Zeeman transition with linewidth of < 5 Hz is observed.

The systematic uncertainty evaluation for both clocks has been made before we give the comparison results here. Most of the frequency shifts were evaluated as our previous work [25,26].

Like most of the optical clocks, for our clocks, the largest frequency shift comes from blackbody radiation (BBR). To evaluate this frequency shift, the precise measurement of the environmental temperature is needed, as well as knowledge of the BBR shift coefficients with a high precision. The theoretical prediction of the coefficient by Safronova and Safronova [31] gives an uncertainty at the 10^{-17} level, which can be achieved with a K-level-uncertainty temperature measurement of the trap environment. For our system, we consider both the temperature variation of the vacuum chamber and the temperature difference of the trap relative

to the vacuum chamber. The temperature of the vacuum chamber has been measured to be 294.2(1.5) K during the experiments. As for the temperature difference of the trap relative to the vacuum chamber, it should be rather small due to the small electrode capacitance and the trap configuration, which has been estimated to have 1.5-K uncertainty by National Research Council of Canada [32] using a similar configuration as our traps. However, several groups have measured the temperature difference with larger uncertainties, using both temperature sensors [1,2] and thermal imaging [3]. With a thermal imaging camera (0.1-K resolution, 1.0-K accuracy) through a MgF_2 window, the temperature difference of an identical trap driven by an rf with twice the amplitude as we used in the experiments was measured to be < 0.5 K before and after the rf field was applied. Considering the solid angle of the electrodes viewed by the ion, as well as the possible temperature difference between the traps, we tested with an imaging camera, and, for the ones we used in the experiments, the average temperature is estimated to be 294.4(1.6) K. The BBR shifts for both clocks are evaluated to be $-354.5(9.4)$ mHz, in which the coefficients contribute 5.2 mHz to the uncertainty, while the temperature measurements contribute 7.8 mHz to the uncertainty.

As for the systematic uncertainties, one of the greatest contributions comes from the excess micromotion; direct observation of ion displacement with an imaging system [18,27] together with observing the resolved micromotion sidebands [27,28] are performed to measure the estimation of the excess micromotion in three directions. In a Paul trap, the ion's position will be shifted due to the electric stray field, and the displacement will be inversely proportional to the depth of the pseudopotential, which can be determined by measuring the secular frequencies. In our case for clock 1, the probe laser is sent into the chamber horizontally, which is $\sim 45^\circ$ angled to both the trap axial direction and the trap ring plane; the camera is located with a detecting direction that is also horizontal and perpendicular to the probe laser k vector and is $\sim 45^\circ$ angled to both the trap axial direction and the trap ring plane. Using an EMCCD-based imaging system with a resolution limit of $5 \mu\text{m}$, no position change can be seen from the camera when the trap rf amplitude is changed with secular frequencies changed from $\omega_x \approx \omega_y = 2\pi \times 1.4(1)$ MHz, $\omega_z = 2\pi \times 2.9(1)$ MHz to $\omega_x \approx \omega_y < 2\pi \times 0.2$ MHz, $\omega_z < 2\pi \times 0.4$ MHz. Thus, the upper limit of the micromotion parallel to the EMCCD sensor can be estimated. Ion displacement perpendicular to the EMCCD sensor will cause micromotion on the k -vector direction of the probe laser beam, which can be estimated with the help of observing the micromotion sideband to carrier intensity ratio. The upper limit of the uncompensated static electric stray field \mathbf{E} is evaluated as $|E_x| < 5.2$ V/m, $|E_y| < 3.4$ V/m, and $|E_z| < 18.9$ V/m. The frequency shift caused by excess micromotion is evaluated to be $-17(17)$ mHz.

TABLE I. Systematic shifts and uncertainties for the evaluations of both the single clocks and the comparison; all the numbers shown are in millihertz.

	Clock 1		Clock 2		Clock 2–clock 1	
	Shift	Uncertainty	Shift	Uncertainty	Shift	Uncertainty
BBR: due to temperature	−354.5	7.8	−354.5	7.8	0.0	2.4
BBR: uncertainty due to Stark constant	...	5.2	...	5.2
Excess micromotion	−17.0	17.0	0.0	4.6	17.0	17.6
Stark–secular motion						
2nd-order Doppler micromotion due to secular motion	−6.7	3.4	0.0	0.3	6.7	3.4
2nd-order Doppler–secular motion	−7.8	3.9	−4.7	2.2	3.1	4.5
ac-Stark −397 nm	0.7	0.7	0.4	0.4	−0.3	0.8
ac-Stark −866 nm	−0.1	0.1	−0.1	0.1	0.0	0.1
ac-Stark −854 nm	−0.1	0.1	−0.1	0.1	0.0	0.1
ac-Stark −729 nm	3.0	3.0	0.3	0.3	−2.7	3.0
Residual quadrupole	0.0	1.6	0.0	1.5	0.0	2.2
Residual 1st-order Zeeman	0.0	0.6	0.0	0.6	0.0	0.8
2nd-order Zeeman	0.1	0.1	0.1	0.1	0.0	0.1
AOM chirping	0.0	0.1	0.0	0.1	0.0	0.1
Line pulling	0.0	0.1	0.0	0.1	0.0	0.1
Collision	0.0	0.1	0.0	0.1	0.0	0.1
1st-order Doppler	0.0	0.1	0.0	0.1	0.0	0.1
Servo	15.9	8.1	16.0	8.0	0.1	8.4
Gravitational shift					0.0	0.4
Total	−367	22	−343	14	24	21

For clock 2, which works at $2\pi \times 24.7(2)$ MHz, the 2nd-order Doppler shift and Stark shift cancel each other; thus, the shift and uncertainty are smaller. Considering both the uncertainty of the micromotion amplitude and the uncertainty of the calculated scalar polarizability [31], a frequency shift of 0.0(4.6) mHz is derived.

The heating rates for both traps have been measured to understand the ion's temperature better and are 0.047(2) mK/ms for clock 1 and 0.024(1) mK/ms for clock 2; the frequency shifts due to secular motion are evaluated according to the measured average temperature. During the experiment, the nonlinear drift of the probe laser causes the software controlled servo to stop following the laser perfectly, which gives rise to a servo shift and uncertainty. The servo shift and uncertainty can be inferred from the residual errors in the quantum jump imbalances. Compared to our previous work [26], the uncertainties caused by the linear Zeeman effect, the quadrupole shift, and the ac-Stark shift due to the probe laser are greatly reduced. When evaluating these shifts, the self-comparison method is used by locking independent servos for two different sets of parameters, which is similar to Ref. [6]. The improvements are due mainly to the better magnetic shielding and higher resolution from the better clock stability.

For the evaluation of the systematic shifts and uncertainties in the frequency comparison of two clocks, most of the above effects are not correlated. However, the uncertainties with common mode are reevaluated, including the BBR shift, the servo error and shift, and the gravitational shift. The two clocks are located on the same optical table,

and the temperature difference of the two vacuum chambers is measured to be smaller than the variation of the room temperature. Thus, the difference of the blackbody radiation shift should be small. Assuming the uncertainty of the average temperature difference is 0.5 K (considering the temperature difference comes from the trap electrodes), the corresponding frequency uncertainty is 2.4 mHz. The height difference for two traps is measured to be within 1 cm. Thus, the gravitational shift difference is $<1 \times 10^{-18}$.

Table I summarizes the above evaluation of the systematic shifts and uncertainties. Both clocks have reached an uncertainty of $<6 \times 10^{-17}$. The uncertainty of the clock comparison is also at $<6 \times 10^{-17}$.

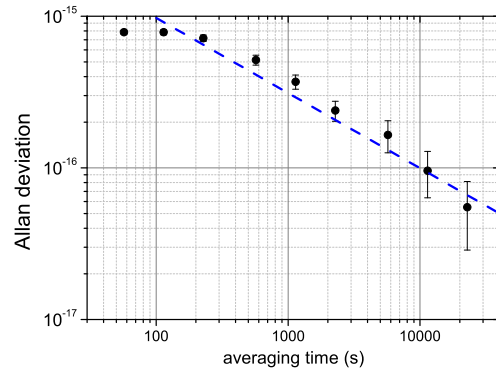


FIG. 1. Standard Allan deviation of the frequency difference between the two $^{40}\text{Ca}^+$ clocks divided by $\sqrt{2}$ to reflect the performance of a single clock. The dashed blue line represents a stability of $1 \times 10^{-14}/\sqrt{\tau}$.

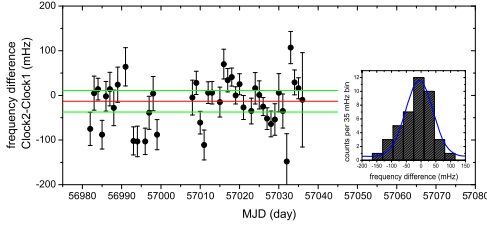


FIG. 2. Frequency comparison of the two clocks. The mean frequency is indicated by the red line and the 3σ uncertainties (σ represents the standard deviation of the mean calculated for the whole data set) by green lines. Inset: A histogram of the individual frequency measurements shown in the figure with a Gaussian fit to show the normally distributed data.

The two clocks are running synchronously; for the longest continuous data sets (>2 days), the Allan deviation of the frequency difference between two clocks is calculated, and the mean result is shown in Fig. 1. Considering the common mode contribution for both clocks is small relative to the total uncertainty, the Allan deviation for the frequency difference between the two $^{40}\text{Ca}^+$ clocks is simply divided by $\sqrt{2}$ to represent the stability for a single clock. During this comparison, the pulse time chosen for the probe laser is 80 ms. The stability is ~ 37 times better than the comparison results of clock 1 and a hydrogen maser in 2012 [26].

The frequency comparison between the two clocks is shown in Fig. 2, where the data set has already been corrected for the systematic shifts described in Table I. The comparison is performed on 42 individual days. Each data point represents an average of the comparison data taken each day, corresponding to 40 000–80 000 s of data. The weighted average frequency difference between the two clocks is $-13(8)$ mHz. Considering the statistical uncertainty (type A) of 8 mHz (1.9×10^{-17}) together with the systematic uncertainty (type B) described in Table I of

21 mHz (5.1×10^{-17}), the total uncertainty for the comparison is 23 mHz (5.5×10^{-17}).

The absolute frequency measurements of the clock transition are performed simultaneously with the comparison. The clock transition frequency of clock 1 is measured using a comb referenced to a hydrogen maser, after which the hydrogen maser is calibrated via GPS referenced to UTC(NIM) using precise point positioning data-processing technique [33]. The frequency offset of UTC(NIM) relative to the SI second can be evaluated through BIPM circular-T reports [34]. The uncertainty budget for the absolute frequency measurements is described in Table II.

The unperturbed center frequency for the clock transition is measured to be 411 042 129 776 401.3 (1.6) Hz in November 2014, 411 042 129 776 401.9 (1.0) Hz in December 2014, and 411 042 129 776 401.7 (1.2) Hz in January 2015, respectively. The averaged mean of the measurements is 411 042 129 776 401.7(1.1) Hz. The uncertainty is mainly limited by the statistical uncertainty from the comb measurements, which is limited by the stability of the hydrogen maser. Beside these measurements, the other one-month measurements in 2012 gave a result of 411 042 129 776 400.5 (1.2) Hz. The recent measurements are in agreement with the measurements in 2012. However, the two measurement sets disagree with the previous published data presented by other groups [21,24] as well as our group [26]. Figure 3 gives an overview of our measurements described in this Letter as well as the ones published earlier and the CIPM-recommended frequency.

After searching for the possible difference in evaluation of the shift and uncertainties, the most probable reason we gave a lower frequency in Ref. [26] is that the micromotion shifts have been underestimated. At a trap drive frequency of $\sim 2\pi \times 9.8$ MHz, the sign of the shifts due to micromotion should be “-.” The micromotion was monitored

TABLE II. Uncertainty budget for the absolute frequency measurements between November 2014 and January 2015; all the numbers shown are in hertz.

	November 2014		December 2014		January 2015			
	Shift	Uncertainty	Shift	Uncertainty	Shift	Uncertainty		
Systematic shifts (Table I)	0.37	0.02	0.37	0.02	0.37	0.02		
Gravitational	1.25	0.05	1.25	0.05	1.25	0.05		
Statistical	...	1.3	...	0.3	...	0.4		
H-maser referenced to UTC(NIM)	187.7	0.5	191.5	0.5	192.1	0.5		
UTC(NIM) referenced to International Atomic Time (TAI)	-0.7	0.8	-0.7	0.8	-0.4	0.9		
TAI referenced to TT(SI)	0.29	0.11	0.22	0.11	0.24	0.16		
Total	188.9	1.6	192.6	1.0	193.5	1.2		
Measurements referenced to H maser	411 042 129 776 590.2		411 042 129 776 594.5		411 042 129 776 595.2			
Unperturbed frequency determined								Average Uncertainty
-411042 129 776 000	401.3	1.6	401.9	1.0	401.7	1.2	401.7	1.1

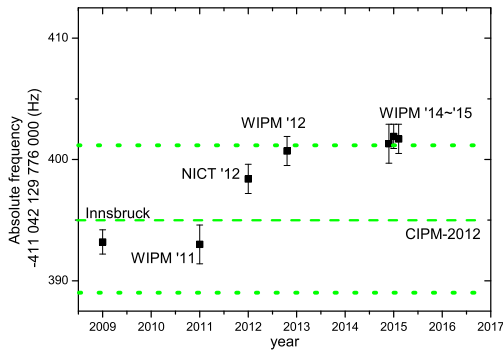


FIG. 3. An overview of the absolute frequency measurements published as well as the data presented in this Letter. The left three data points are the most recent measurements from three individual groups [21,24,26], and the right four data points are the measurement results given in this Letter. The CIPM-recommended frequency including the uncertainty is also shown with green lines in the figure.

only in one direction, and the other two perpendicular directions were unclear. However, in the recent measurements, the micromotion is more carefully minimized and estimated in three directions. Moreover, a specific trapping frequency at $\sim 2\pi \times 24.7$ MHz around which the rf-induced Stark shifts and 2nd-order Doppler shifts cancel each other [2,32] are adopted with clock 2. When operating clock 1 at different confinements of ω_z between $\sim 2\pi \times 1.4$ MHz and $\sim 2\pi \times 0.4$ MHz, the frequency change of clock 1 (taking clock 2 as a reference) is measured to be within the statistical uncertainty of 8×10^{-17} in an experiment lasting for 2 days. Finally, the two clocks that worked under different trapping frequencies give clock transition frequencies that agree with each other at the 10^{-17} level, which further indicates that no large micromotion shifts exist for both clocks in the recent experiments.

In summary, two $^{40}\text{Ca}^+$ optical clocks have been compared over one month with a measurement uncertainty of 5.5×10^{-17} , which is the first-time demonstration of a $^{40}\text{Ca}^+$ optical clock that is better than the Cs fountain primary frequency standards. Besides, the absolute frequency of the clock transition is measured. Based on the evaluation and analysis, the shift caused by the micromotion in one of the two clocks is found to be the dominant factor for the uncertainties for the clock comparison. The maximum probe time and thus the stability of the clocks is limited by the coherence time of the laser and the atom. The coherence time of the atom is limited by the heating rate of the ions in the trap and ac magnetic field fluctuations. The laser stability can be improved as a better design of the magnetic shielding and the traps with lower heating rates, which will increase the coherence time to improve the stability. Future improvement can be made with a new design of the vacuum chambers, which allows better compensation and more precise measurement of the micromotion in three directions and therefore reduces the

uncertainty caused by the micromotion. Furthermore, both traps can work with a driving frequency of $\sim 2\pi \times 24.7$ MHz to further lower the shift. The precise measurement of that frequency will be carried out to improve the uncertainties caused by both the micromotion and the blackbody radiation [28]. Other methods such as all-optical trapping can be also worth trying for getting rid of the micromotion-induced shifts [35]. With a 0.5-K precision measurement of the trap temperature, it is quite possible that the $^{40}\text{Ca}^+$ optical clock can reach a total uncertainty below the 10^{-17} level through the improved experimental measurements.

We thank J. Ye, P. Dubé, C. Chou, A. Hankin, Z. Fang, C. Ye, J. Li, J. Luo, M. Zhan, and J. Yuan for their help and fruitful discussion. We thank Z. Yan, C. Lee, and Y. Zhu for helpful comments on the manuscript. We thank J. Cao, L. Li, L. Chen, Y. Li, and X. Huang for help with the 729 nm laser system. This work is supported by the National Basic Research Program of China (Grant No. 2012CB821301), the National Natural Science Foundation of China (Grants No. 91336211, No. 11034009, No. 11304363, and No. 11474318), and the Chinese Academy of Sciences.

*guanhua@wipm.ac.cn

†klgao@wipm.ac.cn

- [1] C. W. Chou, D. B. Hume, J. C. J. Koelemeij, D. J. Wineland, and T. Rosenband, *Phys. Rev. Lett.* **104**, 070802 (2010).
- [2] A. A. Madej, P. Dubé, Z. Zhou, J. E. Bernard, and M. Gertsch, *Phys. Rev. Lett.* **109**, 203002 (2012).
- [3] G. P. Barwood, G. Huang, H. A. Klein, L. A. M. Johnson, S. A. King, H. S. Margolis, K. Szymaniec, and P. Gill, *Phys. Rev. A* **89**, 050501 (2014).
- [4] N. Huntemann, M. Okhapkin, B. Lipphardt, S. Weyers, Chr. Tamm, and E. Peik, *Phys. Rev. Lett.* **108**, 090801 (2012).
- [5] S. A. King, R. M. Godun, S. A. Webster, H. S. Margolis, L. A. M. Johnson, K. Szymaniec, P. E. G. Baird, and P. Gill, *New J. Phys.* **14**, 013045 (2012).
- [6] B. J. Bloom, T. L. Nicholson, J. R. Williams, S. L. Campbell, M. Bishof, X. Zhang, W. Zhang, S. L. Bromley, and J. Ye, *Nature (London)* **506**, 71 (2014).
- [7] T. L. Nicholson *et al.*, *Nat. Commun.* **6**, 6896 (2015).
- [8] I. Ushijima, M. Takamoto, M. Das, T. Ohkubo, and H. Katori, *Nat. Photonics* **9**, 185 (2015).
- [9] S. Falke *et al.*, *New J. Phys.* **16**, 073023 (2014).
- [10] R. Le Targat *et al.*, *Nat. Commun.* **4**, 2109 (2013).
- [11] J. J. McFerran, L. Yi, S. Meiri, W. Zhang, S. DiManno, M. Abgrall, J. Guena, Y. LeCoq, and S. Bize, *Phys. Rev. A* **89**, 043432 (2014).
- [12] N. Hinkley, J. A. Sherman, N. B. Phillips, M. Schioppo, N. D. Lemke, K. Beloy, M. Pizzocaro, C. W. Oates, and A. D. Ludlow, *Science* **341**, 1215 (2013).
- [13] K. Beloy, N. Hinkley, N. B. Phillips, J. A. Sherman, M. Schioppo, J. Lehman, A. Feldman, L. M. Hanssen, C. W. Oates, and A. D. Ludlow, *Phys. Rev. Lett.* **113**, 260801 (2014).
- [14] R. Li, K. Gibble, and K. Szymaniec, *Metrologia* **48**, 283 (2011).

- [15] S. Weyers, V. Gerginov, N. Nemitz, R. Li, and K. Gibble, *Metrologia* **49**, 82 (2012).
- [16] P. Gill, *Phil. Trans. R. Soc. A* **369**, 4109 (2011).
- [17] F. Riehle, *C.R. Phys.* **16**, 506 (2015).
- [18] T. Schneider, E. Peik, and C. Tamm, *Phys. Rev. Lett.* **94**, 230801 (2005).
- [19] T. Rosenband *et al.*, *Science* **319**, 1808 (2008).
- [20] A. D. Ludlow *et al.*, *Science* **319**, 1805 (2008).
- [21] K. Matsubara, H. Hachisu, Y. Li, S. Nagano, C. Locke, A. Nogami, M. Kajita, K. Hayasaka, T. Ido, and M. Hosokawa, *Opt. Express* **20**, 22034 (2012).
- [22] R. M. Godun, P. B. R. Nisbet-Jones, J. M. Jones, S. A. King, L. A. M. Johnson, H. S. Margolis, K. Szymaniec, S. N. Lea, K. Bongs, and P. Gill, *Phys. Rev. Lett.* **113**, 210801 (2014).
- [23] N. Huntemann, B. Lipphardt, C. Tamm, V. Gerginov, S. Weyers, and E. Peik, *Phys. Rev. Lett.* **113**, 210802 (2014).
- [24] M. Chwalla *et al.*, *Phys. Rev. Lett.* **102**, 023002 (2009).
- [25] Y. Huang, Q. Liu, J. Cao, B. Ou, P. Liu, H. Guan, X. Huang, and K. Gao, *Phys. Rev. A* **84**, 053841 (2011).
- [26] Y. Huang, J. Cao, P. Liu, K. Liang, B. Ou, H. Guan, X. Huang, T. Li, and K. Gao, *Phys. Rev. A* **85**, 030503 (2012).
- [27] D. J. Berkeland, J. D. Miller, J. C. Bergquist, W. M. Itano, and D. J. Wineland, *J. Appl. Phys.* **83**, 5025 (1998).
- [28] P. Dubé, A. A. Madej, Z. Zhou, and J. E. Bernard, *Phys. Rev. A* **87**, 023806 (2013).
- [29] H. Guan, Q. Liu, Y. Huang, B. Guo, W. Qu, J. Cao, G. Huang, X. Huang, and K. Gao, *Opt. Commun.* **284**, 217 (2011).
- [30] K. Numata, A. Kemery, and J. Camp, *Phys. Rev. Lett.* **93**, 250602 (2004).
- [31] M. S. Safronova and U. I. Safronova, *Phys. Rev. A* **83**, 012503 (2011).
- [32] P. Dubé, A. A. Madej, M. Tibbo, and J. E. Bernard, *Phys. Rev. Lett.* **112**, 173002 (2014).
- [33] J. Ray, and K. Senior, *Metrologia* **42**, 215 (2005).
- [34] Bureau International des Poids et Mesures (BIPM), Circular T, November and December 2014, January 2015, http://www1.bipm.org/en/scientific/tai/time_ftp.html.
- [35] P. L. Liu, Y. Huang, W. Bian, H. Shao, H. Guan, Y. B. Tang, C. B. Li, J. Mitroy, and K. L. Gao, *Phys. Rev. Lett.* **114**, 223001 (2015).